Acoustic magnons in the long-wavelength limit: Investigating the Goldstone violation in many-body perturbation theory

Mathias C. T. D. Müller, Christoph Friedrich, and Stefan Blügel
Peter Grünberg Institut and Institute for Advanced Simulation, Forschungszentrum Jülich, 52425 Jülich, Germany

(Received 3 March 2016; revised manuscript received 21 June 2016; published 30 August 2016)

Collective spin excitations in magnetic materials arise from the correlated motion of electron-hole pairs with opposite spins. The pair propagation is described by the transverse magnetic susceptibility, which we calculate within many-body perturbation theory from first principles employing the full-potential linearized augmented-plane-wave formalism. Ferromagnetic materials exhibit a spontaneously broken global rotation symmetry in spin space leading to the appearance of acoustic magnons (zero gap) in the long-wavelength limit. However, due to approximations used in the numerical scheme, the acoustic magnon dispersion exhibits a small but finite gap at Γ. We analyze this violation of the Goldstone mode and present an approach that implements the magnetic susceptibility using a renormalized Green function instead of the Kohn-Sham one. This much more expensive approach shows substantial improvement of the Goldstone-mode condition. In addition, we discuss a possible correction scheme, which involves an adjustment of the Kohn-Sham exchange splitting, which is motivated by the spin-wave solution of the one-band Hubbard model. The new exchange splittings turn out to be closer to experiment. We present corrected magnon spectra for the elementary ferromagnets Fe, Co, and Ni.

DOI: 10.1103/PhysRevB.94.064433

I. INTRODUCTION

Collective spin excitations play a fundamental role for the physical properties of magnetic solids. For example, the specific heat [1] or the macroscopic magnetization [2,3] exhibit a characteristic temperature dependence which can be attributed to the low-energy spin waves (magnons) with excitation energies ranging from a few meV up to a few hundreds meV. Another type of spin excitations are the single-particle spin-flip Stoner excitations. These Stoner excitations give an important contribution to the damping of the magnon mode. To study spin excitations, the central quantity of interest is the transverse magnetic susceptibility, from which the complete excitation spectrum, including single-particle spin-flip Stoner excitations and collective spin-wave modes, can be obtained. The excitations manifest themselves as peaks in the spectral function, which is the central quantity in the scattering cross section measured in neutron-scattering experiments [4–8].

In collinear magnetic systems without spin anisotropy, the global spin polarization can be rotated by a homogeneous magnetic field perpendicular to the magnetization axis without a cost of energy. This corresponds to an acoustic magnon mode with vanishing excitation energy in the long-wavelength limit, a condition which we will refer to as the Goldstone condition.

For a theoretical description of spin dynamics various formalisms have been established. The classical Heisenberg model is a frequently used approach to study the collective spin excitations in systems with localized moments. Its parameters, the Heisenberg exchange parameters, can be obtained from constrained density-functional theory [9,10]. The Goldstone condition is identically fulfilled in this approach. However, single-particle Stoner excitations are missing in the Heisenberg model, and the local-moment approximation is not justified for itinerant electronic systems.

Many-body perturbation theory (MBPT) provides a more general theoretical framework that works for systems with localized moments and for metallic magnets alike. In this theory, single-particle Stoner and collective spin excitations appear simultaneously as poles in the transverse magnetic susceptibility, which describes the correlated motion of an electron-hole pair coupled by an effective electron-electron interaction. First applications to real systems [11–13] employed a tight-binding description. The single-particle propagator and the effective interaction then derive from the same Hamiltonian, and the Goldstone condition is fulfilled by construction.

Parameter-free *ab initio* calculations of the magnetic susceptibility are scarce in the literature due to their large computational cost. Apart from calculations based on MBPT [14–16], another method that is often used is time-dependent density-functional theory (TDDFT) [17–26]. Due to approximations in the numerical scheme, the Goldstone condition is often numerically violated. In TDDFT, the origin of this violation is attributed [23,26] to the fact that the exchange-correlation kernel and the noninteracting magnetic susceptibility are derived from different ground-state calculations. Lounis *et al.* ensure the proper long-wavelength limit of the magnon spectrum by deducing the exchange-correlation kernel from a magnetic sum rule. Based on similar arguments, Rousseau *et al.* [26] construct a correction scheme for the magnetic susceptibility leaving the exchange-correlation kernel unchanged. Buczek *et al.* [18,21] account for the Goldstone violation by setting the smallest eigenvalue of the enhancement matrix equal to zero.

The first studies of itinerant ferromagnets using MBPT were performed by Karlsson and Aryasetiawan [14] employing a model potential for the effective interaction. Kotani and van Schilfgaarde [15] studied spin waves based on quasiparticle self-consistent GW calculations [27–30]. Similar to Ref. [23], they determine the effective interaction from a magnetic sum rule, which ensures fulfillment of the Goldstone condition.

Şaşıoğlu *et al.* [16] performed the first full *ab initio* study of spin-wave spectra within MBPT. In contrast to previous works, the screened interaction was calculated explicitly from the random-phase approximation (RPA). To satisfy the Goldstone condition, they introduced a scaling factor for the screened

interaction which was relatively close to 1 in most cases but could reach 1.5 for bulk nickel, unless the exchange splitting was adjusted to the experimental value as an *ad hoc* correction.

The Goldstone violation in these calculations is more fundamental than in the case of TDDFT. In particular, we argue in this paper that the inconsistency between the free propagator and the RPA screened interaction is to a large degree responsible for the violation. These two quantities derive from different Hamiltonians, the former from the Kohn-Sham density-functional theory solution within the local spin-density approximation (LSDA), and the latter from the GW self-energy [31] with an additional static approximation. We argue that constructing the single-particle propagator from a self-consistent Coulomb-hole screened-exchange (COHSEX) self-energy [31] instead should revoke the inconsistency. In fact, numerical results for the bulk $3d$ transition metals iron, cobalt, and nickel confirm this conjecture. Self-consistently renormalizing the propagator with the COHSEX self-energy substantially reduces the Goldstone violation.

In practice, the application of the COHSEX self-energy is considerably more time consuming than standard LSDA calculations. Therefore, we discuss a correction scheme for the LSDA Green function of ferromagnetic materials. The spin-wave solution of the one-band Hubbard model allows the Goldstone condition to be analyzed in detail. It turns out that the magnetization, the exchange splitting, and the interaction among the electron-hole pairs are intimately connected [32,33]. With this in mind, we propose a correction scheme for the noninteracting susceptibility to resolve the Goldstone violation. We show that the corrected LSDA magnon spectra for the $3d$ transition metals iron, cobalt, and nickel are close to the results obtained from the much more expensive COHSEX approach and with experimental measurements.

The paper is organized as follows. Section II sketches the theoretical formulation of the transverse magnetic susceptibility within MBPT. The details of the calculations and the resulting acoustic magnon spectra are discussed in Sec. III. We present and compare results for bulk Fe, Co, and Ni obtained with the Kohn-Sham LSDA Green function and with a Green function that is self-consistently renormalized with the COHSEX self-energy. Additionally, we present a correction scheme for the LSDA Green function yielding results in good agreement with the more expensive COHSEX approach. Section IV gives a summary.

II. THEORY

We briefly recapitulate the calculation of spin excitations within many-body perturbation theory for a ferromagnetic system with collinear magnetization. In neutron scattering experiments, the incoming neutron beam is circular polarized, creating a magnetic response that exhibits the same sense of rotation as the generating field.

The linear response of the magnetic density at space-time coordinate $(\mathbf{r},t)$ to a change in the external magnetic field at $(\mathbf{r}',t')$ is described by the microscopic transverse magnetic susceptibility

$$R(\mathbf{r},\mathbf{r}';t-t') = \frac{\delta\sigma^+(\mathbf{r},t)}{\delta B^+(\mathbf{r}',t')}. \tag{1}$$

The interacting single-particle Green function

$$G_{\alpha\beta}(\mathbf{r},\mathbf{r}';t-t') = -i\langle\Psi_0|\mathcal{T}[\psi_\alpha(\mathbf{r},t)\psi^\dagger_\beta(\mathbf{r}',t')]|\Psi_0\rangle \tag{2}$$

with the interacting many-body ground state $|\Psi_0\rangle$, the time-ordering operator $\mathcal{T}$, and the Heisenberg field operators $\psi^\dagger_\alpha(\mathbf{r},t)$ and $\psi_\alpha(\mathbf{r},t)$ allows the expectation value of the spin-density operator to be written as

$$\sigma^+(\mathbf{r},t) = -2i\,G_{\downarrow\uparrow}(\mathbf{r},\mathbf{r};-\eta), \tag{3}$$

where η is a positive infinitesimal that ensures the correct time order of the field operators. The factor 2 derives from the spin raising operator $\sigma^+_{\alpha\beta} = \sigma^x_{\alpha\beta} + i\sigma^y_{\alpha\beta} = 2\delta_{\alpha\uparrow}\delta_{\beta\downarrow}$ with the x and y Pauli spin matrices.[1] This reformulation makes Eq. (1) amenable to a treatment within many-body perturbation theory. For the sake of convenience, we continue the derivation in simplified formal notation. A detailed derivation can be found in Ref. [34]. Inserting Eq. (3) into Eq. (1) yields, beside prefactors, the functional derivative $\delta G/\delta B$. By means of the Dyson equation $G^{-1} = G_0^{-1} - \Sigma$ with the electronic self-energy Σ and the single-particle noninteracting Green function G_0 of time-dependent Hartree theory we obtain a Bethe-Salpeter equation for R

$$\begin{aligned} R &= -2i\frac{\delta G}{\delta B} = -2i\frac{\delta}{\delta B}\left(G_0^{-1} - \Sigma\right)^{-1} \\ &= 2iGG\frac{\delta}{\delta B}\left(G_0^{-1} - \Sigma\right) = -2iGG + GG\frac{\delta\Sigma}{\delta G}R, \end{aligned} \tag{4}$$

where it has been used that $G_0^{-1} = i\partial_t - H$ contains the Zeeman term in the Hartree Hamiltonian H, so in simplified notation[2] $\delta G_0^{-1}/\delta B = -1$. The first term of Eq. (4) exhibits poles at the single-particle Stoner excitation energies of the noninteracting mean-field system. The second term describes the correlated propagation of an electron-hole pair with opposite spins. It is responsible for the collective spin-wave poles in the magnetic susceptibility. Additionally, it describes the mixture of these collective excitations with the Stoner excitations. This mixing limits the lifetime of the spin-wave excitations. It also gives rise to a many-body renormalization of the Stoner-excitation continuum.

In practical applications the self-energy has to be approximated as its exact form is unknown. We employ the GW approximation [31]

$$\Sigma_{\alpha\beta}(\mathbf{r},\mathbf{r}';\tau) = iG_{\alpha\beta}(\mathbf{r},\mathbf{r}';\tau)W(\mathbf{r},\mathbf{r}';\tau+\eta), \tag{5}$$

with $\tau = t - t'$ and the screened interaction $W = v + vPW$, which incorporates the bare Coulomb interaction $v(\mathbf{r},\mathbf{r}') = 1/|\mathbf{r}-\mathbf{r}'|$ and screening effects described by the random-phase approximation (RPA) to the polarization function

$$P(\mathbf{r},\mathbf{r}';\tau) = -i\sum_\alpha G_{\alpha\alpha}(\mathbf{r},\mathbf{r}';\tau)G_{\alpha\alpha}(\mathbf{r}',\mathbf{r};-\tau-\eta). \tag{6}$$

[1]The external field $\delta B^+(\mathbf{r}',t') \propto e^{-i\omega t'}$ refers to clockwise circular polarization with respect to the magnetization direction.

[2]To be more precise, $\delta G^{-1}_{0,\alpha\beta}(\mathbf{r},t)/\delta B^+(\mathbf{r}',t') = -g_e\mu_B\sigma^+_{\alpha\beta}\delta(\mathbf{r}-\mathbf{r}')\delta(t-t')/2$ with the electron Landé factor g_e and the Bohr magneton μ_B.

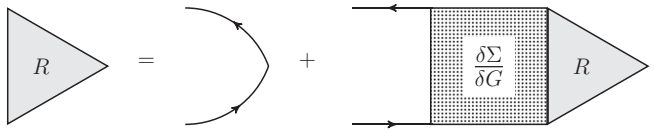

FIG. 1. Representation of Eq. (4) for the transverse magnetic susceptibility in Feynman diagrams. Successive reinsertion of R on the right-hand side and $\delta\Sigma/\delta G = iW$ generates the ladder approximation.

Differentiating Eq. (5) with respect to G formally produces two terms, of which one vanishes in the case of a collinearly polarized system [34], leaving only $\delta\Sigma/\delta G = iW$. We furthermore approximate the dynamical screened interaction to be instantaneous. As a consequence, the Fourier transform is constant in the angular frequency ω, and we set it to its static limit $W(\mathbf{r},\mathbf{r}';\omega) \to W(\mathbf{r},\mathbf{r}';0)$, which seems to be a reasonable approximation since we are mainly interested in the low-energy spin-wave excitations.

While R as defined in Eq. (1) is a two-point function, we have to generalize its definition to a three-point function in Eq. (4) because $\delta G/\delta B$ depends on three points in space and time. Successive reinsertion of R on the right-hand side generates terms of ever increasing order in W, the *ladder approximation*, as shown diagrammatically in Fig. 1. Equation (4) is an integral equation, which can be made into a matrix equation by expansion in a product basis $\{w_\mu(\mathbf{r})w^*_\nu(\mathbf{r}')\}$ with $\{\mu,\nu\}$ as a composite index to be defined below. We also perform the Fourier transformation $\tau \to \omega$. The magnetic susceptibility then turns into a four-point quantity $R^{(4)}$, and Eq. (4) can be solved by matrix inversion

$$R^{(4)} = (1 - KW)^{-1}K \tag{7}$$

defining the two-particle free propagator as $K = iGG$. Both quantities, $R^{(4)}$ and K, depend on four points in space and one frequency argument. The original two-point magnetic susceptibility of Eq. (1) is obtained by contraction

$$R(\mathbf{r},\mathbf{r}';\omega) = -2R^{(4)}(\mathbf{r},\mathbf{r};\mathbf{r}',\mathbf{r}';\omega). \tag{8}$$

For a comparison with measured spectral functions, one can project the imaginary part onto the plane wave $e^{i\mathbf{q}r}$ from both sides, which gives the function $\mathrm{Im}R(\mathbf{q},\omega)$. Peaks in this function correspond to spin excitations, where well-defined collective excitations, the spin waves, manifest themselves as sharp δ-like peaks. Plotting the respective ω values against $\mathbf{q}$ yields the magnon dispersion relation.

In the present paper, we focus on the long-wavelength limit of the spin-wave excitation spectrum. The Goldstone theorem states that the spontaneously broken spin-rotation symmetry in ferromagnetic materials leads to the appearance of a gapless magnon dispersion curve, i.e., the excitation energy vanishes in the limit $\mathbf{q} \to 0$. This has a very simple physical explanation. In the limit $\mathbf{q} \to 0$, the generating field is a homogeneous magnetic perturbation perpendicular to the ferromagnetic spin alignment. The $\mathbf{B}$ field acts to rotate all electron spins collectively towards the field direction. In the absence of spin-orbit coupling this rotation can take place without a cost of energy; hence $\omega = 0$. However, in practical *ab initio* calculations this simple condition is often violated. We analyze the Goldstone violation in the next section and discuss possible solutions.

III. CALCULATIONS

The implementation of the transverse magnetic susceptibility is realized in the SPEX code [35] and relies on the full-potential linearized augmented-plane-wave (FLAPW) method. The mean-field solution that serves as the starting point for MBPT is provided by the FLEUR code [36], which is a FLAPW implementation of density-functional theory (DFT) [37,38]. The functions $w_\mu(\mathbf{r})$ forming the product basis, see above, have to fulfill two conditions. First, they should be localized at atomic sites to enable an efficient truncation of the numerically small off-site contributions [16,34], and, second, they should be chosen such that the energetic subspace one aims to describe is reproduced properly. As spin-wave excitations are mainly driven by the electronic d states located around the Fermi level, it is that energy region which is of importance to the magnetic response function. In other words, the set of Wannier functions must couple to the relevant hole and electron Green function that attach to the vertices of the four-point quantities. To fulfill these two conditions, we employ for each material a set of nine maximally localized Wannier functions [39,40] of s, p, and d orbital character, which are constructed from the 18 energetically lowest mean-field single-particle states $\varphi^\sigma_{\mathbf{k}n}(\mathbf{r})$ with Bloch momentum $\mathbf{k}$, band index n, and spin σ. We have also tested two sets that are formed from the 12 and 24 energetically lowest states, respectively, yielding very similar results. On the one hand, the number of bands should not be too small to guarantee an adequate description of the electron propagator (which is built from empty states). On the other hand, one has to make sure that the Wannier set still represents the low-energy electronic bands sufficiently accurately. To this end, the number of bands used in the Wannier construction should not exceed the number of Wannier functions too much. The *Wannier product basis* is used to represent $R^{(4)}$, K, and W as matrices, allowing Eq. (7) to be solved by matrix inversion.

The screened interaction is first calculated within the mixed product basis [35,41] before it is projected onto the Wannier product basis. The two-particle propagator $K = iGG$ is directly evaluated in the Wannier product basis utilizing the Lehmann representation of the Green function [16,34].

The many-body calculation of spin excitations is a multistage process. The first step is a self-consistent-field calculation of the electronic ground state within DFT, where we employ the local-spin-density approximation (LSDA) for the exchange-correlation energy functional in the parametrization by Perdew and Zunger [42]. The calculations are performed with the lattice constants 2.87 Å, 3.54 Å, and 3.53 Å for Fe, Co, and Ni, respectively. The Brillouin zone (BZ) is sampled with a $14\times14\times14$ $\mathbf{k}$-point grid for all calculations. For the BZ integrations we employ the tetrahedron method [43].

In the following, we discuss the spin-wave spectra for the elementary bulk ferromagnets Fe, Co, and Ni with regard to the starting-point dependence of MBPT. We refer here to the Green function with which the two-particle propagator K is calculated. Since a set of single-particle states is already

available from the ground-state calculation, a convenient choice is the LSDA Green function calculated from the corresponding Kohn-Sham wave functions and energies. The resulting spin-wave dispersions for all three materials are shown as blue triangles in Fig. 3, correctly showing a quadratic behavior around the Γ point. However, they also clearly exhibit a gap error: the spin-wave excitation energy does not vanish in the center of the BZ as it should.

There are a number of possible reasons for this violation. The most obvious among them are the approximations applied in our numerical approach. For example, we have employed an on-site approximation. While the electron-hole pair can propagate over arbitrarily many lattice sites, they are not allowed to separate further than one lattice site, i.e., we expect the electron and hole to be on the same site for all times. In other words, the screened interaction is assumed to fall off sufficiently fast so that off-site contributions can be neglected. The assumption of a short-range interaction seems to be justified for the metallic systems considered in this work. The nearest-neighbor interactions are found to be typically 98% smaller than the corresponding on-site terms. Second, the choice of the Wannier basis effectively restricts the band summation for the Green function to those bands that are used in the construction of the Wannier functions (18 bands). Related to this, the corresponding Wannier product basis might be inadequate for representing plane waves with small Bloch vectors, in particular the constant function relevant for the Goldstone limit $\mathbf{q} \to 0$. Finally, convergence issues ($\mathbf{k}$-point set, basis sets, empty-state summations, etc.) might be partly responsible for the gap error.

In contrast to these issues related to the numerical realization, there is another more fundamental inconsistency in the chosen approach, which we will investigate in the following. This inconsistency concerns the choice of the starting point, i.e., the LSDA Green-function propagator. Equation (7) is derived under the assumption that the Green function is renormalized with the self-energy Σ since it appears as the solution of the Dyson equation in Eq. (4). Furthermore, when evaluating the functional derivative $\delta\Sigma/\delta G$ with Eq. (5) for the self-energy, we implicitly assume G to be self-consistently renormalized with the GW self-energy. Only if these conditions are fulfilled do we obtain the infinite series of ladder diagrams shown in Fig. 1. This relationship is also apparent in the form of Eq. (7). For a pole to appear in the Goldstone limit, at least one eigenvalue of the matrix $1 - KW$ must vanish exactly for $\mathbf{q} \to 0$ and $\omega \to 0$. This is obviously not possible with arbitrary combinations of W and K, which in turn depends on the choice of the Green function through $K = -iGG$. The two quantities, G and W, are thus related, and one must be chosen in accordance with the other. The fact that the screened interaction itself depends on G through the RPA approximation [Eq. (6)] could lead one to believe that a consistent choice would be to generate K and W from the same G. This is not so since the particular construction of W never enters the derivation of Eq. (7). In this sense, the screened interaction appears merely as a parameter, and G has to be chosen in accordance with W for the Goldstone condition to be fulfilled.

As a consequence, to remain consistent with the underlying theory, we must choose the Green function to be one that is self-consistently renormalized with the self-energy Eq. (5). Unfortunately, fully self-consistent GW calculations for transition-metal bulk systems are nowadays still a major challenge due to the dense $\mathbf{k}$-point sets that are needed. On a second thought, however, we should also remember the static approximation that we have applied to the screened interaction. For this reason, the proper self-energy to be used in the framework of our theoretical approach would have to be constructed with the static screened interaction. An obvious choice would be the screened-exchange (SEX) self-energy, in which the dynamical W of Eq. (5) is replaced by an instantaneous interaction, whose Fourier transform would be the static $W(\mathbf{r},\mathbf{r}') = W(\mathbf{r},\mathbf{r}';\omega = 0)$, corresponding to Hartree-Fock theory with the bare Coulomb interaction replaced by $W(\mathbf{r},\mathbf{r}')$

$$\Sigma^{\sigma}_{\mathrm{SEX}}(\mathbf{r},\mathbf{r}') = -\sum_{\mathbf{k}}^{\mathrm{BZ}}\sum_{n}^{\mathrm{occ}} \varphi^{\sigma}_{\mathbf{k}n}(\mathbf{r})\varphi^{\sigma\,*}_{\mathbf{k}n}(\mathbf{r}')W(\mathbf{r},\mathbf{r}'). \qquad (9)$$

It is known however that the so-defined SEX self-energy is not a good approximation. In fact, the static limit [31] of the GW self-energy not only involves the SEX term but also an additional Coulomb-hole (COH) contribution

$$\Sigma^{\sigma}_{\mathrm{COH}}(\mathbf{r},\mathbf{r}') = \tfrac{1}{2}\delta(\mathbf{r}-\mathbf{r}')[W(\mathbf{r},\mathbf{r}') - v(\mathbf{r},\mathbf{r}')], \qquad (10)$$

which acts as a local and spin-independent potential. It accounts for the interaction energy of a quasiparticle with its induced (static) polarization cloud. Therefore, this term only couples charge degrees of freedom (if spin-orbit coupling is set aside) and does not affect the linear response of transversal spin fluctuations. Only the SEX self-energy [Eq. (9)], corresponding to Eq. (5) with $W(\mathbf{r},\mathbf{r}';\tau+\eta)$ replaced by $W(\mathbf{r},\mathbf{r}')$, contributes to the right-hand side of Eq. (4) with $\delta\Sigma/\delta G = iW(0)$. Obviously, this leads to the same form of the Bethe-Salpeter equation [Eq. (7)] as before. Furthermore, an additional static approximation of the screened interaction is not needed anymore since the static limit is already taken in the COHSEX self-energy.

To obtain the properly renormalized electronic Green function, we must solve the Dyson equation self-consistently with the COHSEX self-energy. Technically, we start from the mean-field LSDA solution and construct the LSDA Green function, the corresponding polarization function [Eq. (6)], and the static screened interaction $W = v + vPW = (1 - vP)^{-1}v$, from which the COHSEX self-energy $\Sigma^{\sigma}_{\mathrm{SEX}} + \Sigma^{\sigma}_{\mathrm{COH}}$ is evaluated. The latter is a Hermitian operator defining a new mean-field system. This allows the respective single-particle equations of motion (quasiparticle equations) to be solved in a similar way as the Kohn-Sham equations of DFT. To be more precise, the single-particle equations are iteratively solved until the density is converged. This process updates the density and, consequently, the local effective potential in each iteration while the COHSEX self-energy matrix remains fixed. This produces a new set of wave functions and energies that are then used to construct a new Green function and, ultimately, a new COHSEX self-energy matrix, etc. The whole procedure is repeated until self-consistency is achieved.

The mean-field solution of the 3d ferromagnets bcc iron, fcc cobalt, and fcc nickel based on the COHSEX self-energy is interesting in its own right. Figure 2 shows the density of states

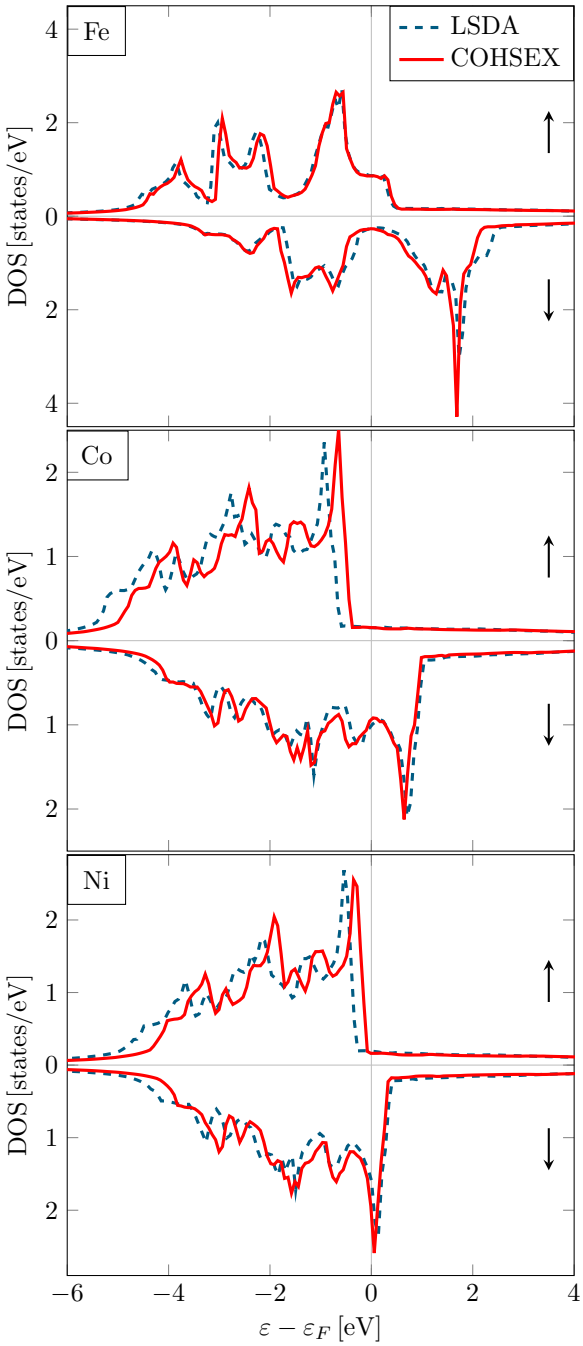

FIG. 2. DOS spectra for the bulk 3*d* transition metals iron, cobalt, and nickel. The upper and the lower panel show the majority and the minority spin channel, respectively. The Fermi level is set to zero.

(DOS) for Fe, Co, and Ni for both LSDA and COHSEX. At first glance, the two DOS spectra look very similar for all materials. The COHSEX self-energy yields thus qualitatively the same correct result as LSDA: all three materials are ferromagnetic metals. There are however slight quantitative changes. The occupied band width shrinks, in particular for Co and Ni, and the spin-up and spin-down states show a relative energetic shift to smaller values. This observation is confirmed by the exchange splittings of selected single-particle states listed in Table I. The COHSEX values are systematically smaller than

TABLE I. Spin magnetic moments m and exchange splittings E_{ex} for selected states calculated within LSDA and COHSEX as well as corrected LSDA and corresponding experimental values for Fe, Co, and Ni.

			LSDA	LSDA corr.	COHSEX	Experiment
m (μ_{B})	Fe		2.20	2.16	2.11	2.08 [44,45]
	Co		1.62	1.49	1.46	1.52 [44,45]
	Ni		0.59	0.51	0.46	0.52 [44,45]
E_{ex} (eV)	Fe	Γ'_{25}	1.8	1.7	1.5	2.1 [46–49]
		H_{25}	2.1	2.0	1.7	1.8 [49]
		P_4	1.4	1.3	1.1	1.5 [50]
	Co	Γ_{12}	1.7	1.3	1.1	1.1 [51]
		Γ'_{25}	1.4	1.0	1.2	1.1 [51]
	Ni	L_3	0.5	0.3	0.4	0.3 [50]
		X_2	0.6	0.4	0.3	0.2 [52]

the LSDA ones, to the effect that the slight overestimation of the magnetic moment found in LSDA is corrected to smaller values in COHSEX, albeit somewhat too strongly in the case of Co and Ni. With the exception of iron, the exchange splittings are improved by the self-consistent COHSEX calculation, most notably for Ni, whose exchange splitting is known to be overestimated in LSDA.

Figure 3 shows the spin-wave dispersion calculated from the COHSEX Green function as red crosses. Employing the self-consistent COHSEX mean-field solution as starting point, in fact, decreases the gap error systematically compared to the corresponding LSDA values. In case of bcc iron, fcc cobalt, and fcc nickel the error is reduced by 85%, 69%, and 79%, respectively; see Table II. As a comparison, we also show results obtained with the Perdew, Burke, and Ernzerhof (PBE) [53] generalized gradient approximation for the exchange-correlation functional, which yields even larger gap errors than LSDA.

The ansatz presented so far is computationally very demanding. It requires the self-consistent calculation of the COHSEX self-energy on a fine **k**-point set as a prerequisite. On the other hand, aside from the gap error, the magnon dispersions obtained from LSDA are very similar to the corresponding COHSEX results (see Fig. 3). This raises the question if it is possible to correct the LSDA Green function in a way that respects the Goldstone condition. In fact, this is possible.

Our approach is motivated by studying spin-wave solutions [32,33] of the one-band Hubbard model, which allows the Goldstone condition to be analyzed and understood in detail. When solved in the Hartree-Fock approximation, we obtain the magnetic susceptibility as a simple algebraic expression in the same form as Eq. (7) with the W matrix replaced by the Hubbard (on-site) interaction parameter U. In the Goldstone limit, the two-particle propagator simplifies to $K = m/E_{\mathrm{ex}}$ with the site magnetization m and the exchange splitting E_{ex}, and the Goldstone condition can be phrased in the form of the simple relation

$$1 = \frac{Um}{E_{\mathrm{ex}}}. \tag{11}$$

To remain consistent, we have to evaluate K in the Hartree-Fock mean-field system, in which case $E_{\mathrm{ex}} = Um$, and the

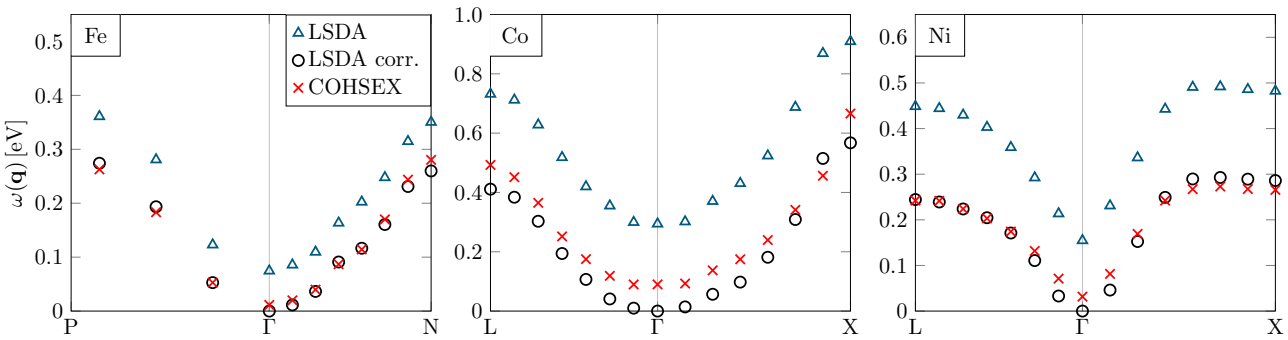

FIG. 3. Spin-wave spectra for Fe, Co, and Ni obtained with the LSDA (blue triangles), corrected LSDA (black circles), and COHSEX (red crosses) Green function as starting points. The spin-wave dispersion is shown along the high-symmetry line P → Γ → N and L → Γ → X for the bcc and fcc structures, respectively.

Goldstone condition is identically fulfilled. The simple form of the relation invites one to use one of the constituent quantities as an adjustable parameter. The U parameter plays the role of the screened interaction W, which is a matrix and thus cannot be corrected easily by a single parameter. Besides, we obtain W from a many-body treatment of screening, and it does not seem to be appropriate to correct it in such an *ad hoc* way. Second, the magnetization m results from the self-consistent LSDA calculation and cannot be varied straightforwardly. At last, E_{ex} can be regarded as the energy difference between the spin-up and spin-down electron bands. This band alignment can easily be varied once a self-consistent LSDA solution has been found. Moreover, this will specifically modify the LSDA Green function, which was our intention, while leaving the screened interaction unchanged. This correction can be hoped to mimic to some extent the missing renormalization in the Green function. Therefore, we choose E_{ex} as an adjustable parameter. To be more precise, we rigidly shift the spin-up and spin-down states relative to each other

$$\tilde{\epsilon}^{\uparrow/\downarrow}_{\mathbf{k}m} = \epsilon^{\uparrow/\downarrow}_{\mathbf{k}m} \pm \frac{\Delta E_{\mathrm{ex}}}{2} \tag{12}$$

until the Goldstone condition is fulfilled. The LSDA Green function corrected in this way is then used to construct the two-particle propagator K, which after insertion into Eq. (4) gives the spin excitations. We note that Refs. [14] and [16] already discuss an adjustment of the exchange splitting, which was however intended as an *ad hoc* correction applied manually to fit to the experiment. Reference [16] anticipates that a self-consistent scheme would bring about a correction of the exchange splitting, which is indeed confirmed by the present results.

This procedure yields magnon dispersions, which respect the Goldstone condition and are close to the COHSEX results for the three materials as shown in Fig. 3. The relative shift in the band energies is such that the exchange splittings decrease. For Fe, Co, and Ni, we find $\Delta E_{\mathrm{ex}} = 0.10$ eV, $\Delta E_{\mathrm{ex}} = 0.39$ eV, and $\Delta E_{\mathrm{ex}} = 0.21$ eV. The Fermi energy is adjusted accordingly so that the correction affects the ground-state magnetic properties as well. Interestingly, the resulting magnetic moments and exchange splittings turn out to be very close to the corresponding COHSEX values listed in Table I. They also compare well with experiment. The proximity of COHSEX and corrected LSDA values can be regarded as an *a posteriori* justification of the correction of Eq. (12).

TABLE II. Starting-point dependence of the spin-wave gap error $\delta\omega$ in the Goldstone limit $\mathbf{q} \to 0$ for Fe, Co, and Ni.

	$\delta\omega_{\mathrm{LSDA}}$ (meV)	$\delta\omega_{\mathrm{GGA}}$ (meV)	$\delta\omega_{\mathrm{COHSEX}}$ (meV)
Fe	75	289	11
Co	294	457	90
Ni	155	242	32

Among the three materials, fcc cobalt appears as a problematic case. The gap error is largest (see Table II) and the COHSEX spin-wave dispersion shows an unusually flat behavior at the Γ point. In fact, the curvature there is very small, being between results from LSDA (small positive curvature) and PBE (small negative curvature, not shown), indicative of a magnetic instability. This is in accordance with previous DFT results. Janak [54] found that there are two competing magnetic ground states with low and high magnetic moment, and Moruzzi *et al.* [55,56] report an unusually strong dependence of the magnetic properties on the lattice constant.

The LSDA gap error was already discussed in Ref. [16], where, as a pragmatic approach, the Goldstone condition was enforced by a simple scaling of the screened interaction $W \to \lambda W$. The screened interaction is $\mathbf{q}$ independent because of the on-site approximation so that the correction affects the spin-wave dispersion throughout the Brillouin zone. Technically, the scaling of W is a simple *a posteriori* correction, while the adjustment of E_{ex} requires the Fermi energy and, thus, the Green function to be recalculated in an iterative way. On the other hand, as already discussed above, there is no real theoretical justification for the scaling of the RPA screened interaction, adopted in Ref. [16] as a simple pragmatic correction. Still, it is worthwhile to see to what extent the resulting spin-wave dispersions will differ. A comparison is shown in Fig. 4, in addition to experimental data obtained from neutron scattering measurements. In fact, the theoretical curves are rather similar with the exception of Ni, where the spin-wave dispersion obtained from the adjustment of the exchange splitting is closer to experiment, in accordance with previous results [14,16]. Furthermore, for Ni and, to a lesser degree, for Co the scaling of W tends to yield stiffer spin-wave dispersions.

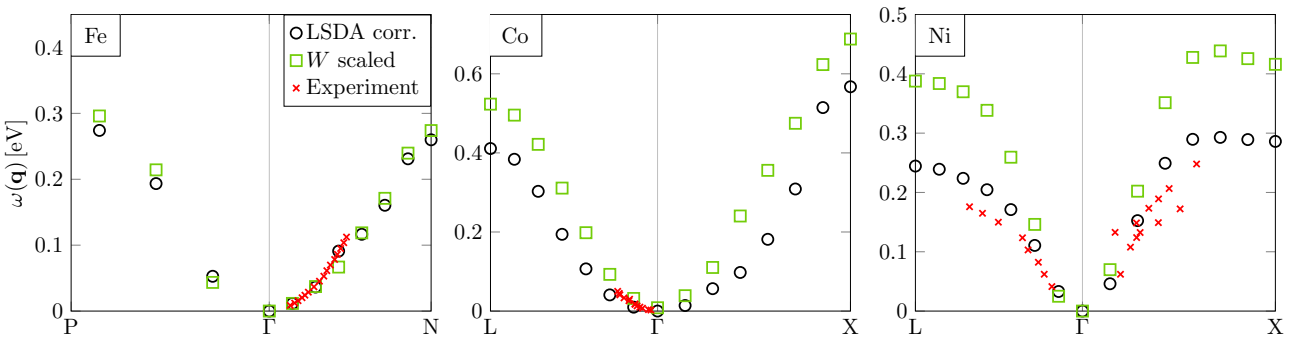

FIG. 4. Spin-wave dispersions that have been calculated using two different Goldstone correction schemes: LSDA corr. as explained in the text and by scaling of W as suggested in Ref. [16]. Experimental values taken from Refs. [57–59] are shown for comparison.

The findings of the present paper can be interpreted in a more fundamental way. Formally, the Hamiltonian which describes the magnetic system is invariant with respect to spin rotations, while the ferromagnetic ground state is not. This implies the existence of a gapless excitation due to a homogeneous magnetic perturbation perpendicular to the magnetization axis. Kadanoff and Baym [60,61] formulated a conserving and self-consistent scheme for correlation functions. The scheme was extended by Brandt *et al.* [62–64] to the magnetic case. They showed that for a spin-conserving formulation of the magnetic susceptibility, which fulfills the Goldstone theorem automatically, several conditions have to be fulfilled. The chosen self-energy approximation is to be calculated self-consistently with the Green function. This ensures that the single-particle states which form the basis for the electron-hole propagator are consistent with the applied self-energy approximation. In addition, the spin-independent interaction that is responsible for the correlation among the electron-hole pairs with opposite spins is required to be consistent with the self-energy as these properties are connected via $\delta\Sigma/\delta G = iW$. If both conditions are fulfilled, the magnetic response function will fulfill the Goldstone theorem. Then, the electron-hole pair propagator and the screened interaction are compatible with the Ward identity ensuring spin conservation. In particular, the correct limit $\mathbf{q} \to 0$ is attained as we have seen in the present work.

IV. CONCLUSIONS

In this paper, we have studied the long-wavelength limit of the spin-wave spectra for the bulk $3d$ transition metals Fe, Co, and Ni from a many-body perturbation theory (MBPT) perspective within the all-electron full-potential linearized augmented-plane-wave (FLAPW) method. The transverse magnetic susceptibility calculated from first principles employing the ladder approximation allows the single-particle Stoner excitations and the collective spin-wave excitations to be accessed simultaneously. The long-wavelength limit is of special interest as the Goldstone theorem demands the existence of a gapless excitation in ferromagnetic materials (neglecting spin anisotropy). Usually, this *Goldstone condition* is numerically violated in practical calculations from first principles.

We have shown in this paper that the gap error is substantially reduced when using the COHSEX Green function instead of the LSDA one. Furthermore, the self-consistent COHSEX calculations give rise to an overall reduction of the exchange splitting compared to LSDA, often leading to better agreement with experiment.

The spin-wave solution of the one-band Hubbard model employing the Hartree-Fock approximation motivates a correction scheme for the LSDA Green function, where the exchange splitting of the Kohn-Sham system is adjusted so as to enforce the Goldstone condition. The resulting spin-wave dispersions are closer to the corresponding COHSEX than to the original LSDA results. The same can be said about the magnetic moments and exchange splittings obtained from the COHSEX and the corrected LSDA Green function, which are found to be very similar, while the original LSDA values are a bit off.

As a result, the corrected LSDA Green function mimics that of the self-consistent COHSEX calculation and is made to fulfill the Goldstone condition exactly, while the numerical cost is identical to a treatment within LSDA. This opens up the possibility of efficient first-principles MBPT calculations of spin excitations that respect the Ward identity of spin conservation. We intend to apply this scheme in the future to the calculation of the electron-magnon scattering within the GT self-energy.

ACKNOWLEDGMENT

The authors acknowledge valuable discussions with Ersoy Şaşıoğlu, Markus Betzinger, Manuel dos Santos Dias, Ferdi Aryasetiawan, and Hans Lustfeld as well as funding from the Deutsche Forschungsgemeinschaft through the Research Training Group 1995 “Quantum Many-Body Methods in Condensed Matter Systems”.

[1] S. Doniach and S. Engelsberg, Phys. Rev. Lett. **17**, 750 (1966).
[2] T. Moriya and A. Kawabata, J. Phys. Soc. Jpn. **34**, 639 (1973).
[3] T. Moriya, *Spin Fluctuations in Itinerant Electron Magnetism* (Springer, Berlin, 1985).

[4] S. W. Lovesey and D. E. Rimmer, Rep. Prog. Phys. **32**, 333 (1969).
[5] R. Lowde and C. Windsor, Adv. Phys. **19**, 813 (1970).
[6] R. D. Lowde, R. M. Moon, B. Pagonis, C. H. Perry, J. B. Sokoloff, R. S. Vaughan-Watkins, M. C. K. Wiltshire, and J. Crangle, J. Phys. F **13**, 249 (1983).
[7] S. W. Lovesey, *Theory of Neutron Scattering from Condensed Matter - Nuclear Scattering* (Clarendon Press, Oxford, 1986).
[8] S. W. Lovesey, *Theory of Neutron Scattering from Condensed Matter - Polarization Effects and Magnetic Scattering* (Clarendon Press, Oxford, 1986).
[9] S. V. Halilov, A. Y. Perlov, P. M. Oppeneer, and H. Eschrig, Europhys. Lett. **39**, 91 (1997).
[10] S. V. Halilov, H. Eschrig, A. Y. Perlov, and P. M. Oppeneer, Phys. Rev. B **58**, 293 (1998).
[11] J. F. Cooke, Phys. Rev. B **7**, 1108 (1973).
[12] J. F. Cooke, J. W. Lynn, and H. L. Davis, Phys. Rev. B **21**, 4118 (1980).
[13] J. F. Cooke, J. A. Blackman, and T. Morgan, Phys. Rev. Lett. **54**, 718 (1985).
[14] K. Karlsson and F. Aryasetiawan, J. Phys.: Condens. Matter **12**, 7617 (2000).
[15] T. Kotani and M. van Schilfgaarde, J. Phys.: Condens. Matter **20**, 295214 (2008).
[16] E. Şaşıoğlu, A. Schindlmayr, C. Friedrich, F. Freimuth, and S. Blügel, Phys. Rev. B **81**, 054434 (2010).
[17] S. Y. Savrasov, Phys. Rev. Lett. **81**, 2570 (1998).
[18] P. Buczek, Ph.D. thesis, Martin-Luther-Universität Halle Wittenberg, 2009.
[19] P. Buczek, A. Ernst, P. Bruno, and L. M. Sandratskii, Phys. Rev. Lett. **102**, 247206 (2009).
[20] P. Buczek, A. Ernst, and L. M. Sandratskii, Phys. Rev. Lett. **106**, 157204 (2011).
[21] P. Buczek, A. Ernst, and L. M. Sandratskii, Phys. Rev. B **84**, 174418 (2011).
[22] S. Lounis, A. T. Costa, R. B. Muniz, and D. L. Mills, Phys. Rev. Lett. **105**, 187205 (2010).
[23] S. Lounis, A. T. Costa, R. B. Muniz, and D. L. Mills, Phys. Rev. B **83**, 035109 (2011).
[24] S. Lounis, M. dos Santos Dias, and B. Schweflinghaus, Phys. Rev. B **91**, 104420 (2015).
[25] M. dos Santos Dias, B. Schweflinghaus, S. Blügel, and S. Lounis, Phys. Rev. B **91**, 075405 (2015).
[26] B. Rousseau, A. Eiguren, and A. Bergara, Phys. Rev. B **85**, 054305 (2012).
[27] S. V. Faleev, M. van Schilfgaarde, and T. Kotani, Phys. Rev. Lett. **93**, 126406 (2004).
[28] M. van Schilfgaarde, T. Kotani, and S. Faleev, Phys. Rev. Lett. **96**, 226402 (2006).
[29] T. Kotani, M. van Schilfgaarde, and S. V. Faleev, Phys. Rev. B **76**, 165106 (2007).
[30] T. Kotani, M. van Schilfgaarde, S. V. Faleev, and A. Chantis, J. Phys.: Condens. Matter **19**, 365236 (2007).
[31] L. Hedin, Phys. Rev. **139**, A796 (1965).
[32] J. A. Hertz and D. M. Edwards, J. Phys. F **3**, 2174 (1973).
[33] D. M. Edwards and J. A. Hertz, J. Phys. F **3**, 2191 (1973).
[34] C. Friedrich, E. Şaşıoğlu, M. Müller, A. Schindlmayr, and S. Blügel, in *First Principles Approaches to Spectroscopic Properties of Complex Materials*, edited by C. Di Valentin, S. Botti, and M. Cococcioni, Topics in Current Chemistry Vol. 347 (Springer, Berlin, 2014), pp. 259–301.
[35] C. Friedrich, S. Blügel, and A. Schindlmayr, Phys. Rev. B **81**, 125102 (2010).
[36] http://www.fleur.de
[37] P. Hohenberg and W. Kohn, Phys. Rev. **136**, B864 (1964).
[38] W. Kohn and L. J. Sham, Phys. Rev. **140**, A1133 (1965).
[39] N. Marzari and D. Vanderbilt, Phys. Rev. B **56**, 12847 (1997).
[40] A. A. Mostofi, J. R. Yates, Y.-S. Lee, I. Souza, D. Vanderbilt, and N. Marzari, Comput. Phys. Commun. **178**, 685 (2008).
[41] C. Friedrich, M. Betzinger, M. Schlipf, S. Blügel, and A. Schindlmayr, J. Phys.: Condens. Matter **24**, 293201 (2012).
[42] J. P. Perdew and A. Zunger, Phys. Rev. B **23**, 5048 (1981).
[43] J. Rath and A. J. Freeman, Phys. Rev. B **11**, 2109 (1975).
[44] M. B. Stearns, in *Magnetic Properties in Metals*, edited by H. Wijn and Landolt-Börnstein, Vol. III of New Series (Springer, Berlin, 1986).
[45] D. Bonnenberg, K. Hempel, and H. Wijn, in *Magnetic Properties in Metals*, edited by H. Wijn and Landolt-Börnstein, Vol. III of New Series (Springer, Berlin, 1986).
[46] A. M. Turner, A. W. Donoho, and J. L. Erskine, Phys. Rev. B **29**, 2986 (1984).
[47] E. Kisker, K. Schröder, W. Gudat, and M. Campagna, Phys. Rev. B **31**, 329 (1985).
[48] Y. Sakisaka, T. Rhodin, and D. Mueller, Solid State Commun. **53**, 793 (1985).
[49] A. Santoni and F. J. Himpsel, Phys. Rev. B **43**, 1305 (1991).
[50] D. E. Eastman, F. J. Himpsel, and J. A. Knapp, Phys. Rev. Lett. **44**, 95 (1980).
[51] F. J. Himpsel and D. E. Eastman, Phys. Rev. B **21**, 3207 (1980).
[52] R. Raue, H. Hopster, and R. Clauberg, Z. Phys. B **54**, 121 (1984).
[53] J. P. Perdew, K. Burke, and M. Ernzerhof, Phys. Rev. Lett. **77**, 3865 (1996).
[54] J. Janak, Solid State Commun. **25**, 53 (1978).
[55] P. Marcus and V. Moruzzi, Solid State Commun. **55**, 971 (1985).
[56] V. L. Moruzzi, P. M. Marcus, K. Schwarz, and P. Mohn, Phys. Rev. B **34**, 1784 (1986).
[57] J. W. Lynn, Phys. Rev. B **11**, 2624 (1975).
[58] R. N. Sinclair and B. N. Brockhouse, Phys. Rev. **120**, 1638 (1960).
[59] H. A. Mook and D. M. Paul, Phys. Rev. Lett. **54**, 227 (1985).
[60] G. Baym and L. P. Kadanoff, Phys. Rev. **124**, 287 (1961).
[61] G. Baym, Phys. Rev. **127**, 1391 (1962).
[62] U. Brandt, W. Pesch, and L. Tewordt, Z. Phys. **238**, 121 (1970).
[63] U. Brandt, Z. Phys. **244**, 217 (1971).
[64] U. Brandt, H. Lustfeld, W. Pesch, and L. Tewordt, J. Low Temp. Phys. **4**, 79 (1971).